AIP Journal of Applied Physics

Effect of low-temperature annealing on the luminescent lifetime and negative differential resistance of silicon-implanted borosilicate glass

Gong-Ru Lin

Citation: Journal of Applied Physics **94**, 7542 (2003); doi: 10.1063/1.1630366
View online: http://dx.doi.org/10.1063/1.1630366
View Table of Contents: http://scitation.aip.org/content/aip/journal/jap/94/12?ver=pdfcov
Published by the AIP Publishing

Articles you may be interested in

Effect of annealing on the structural and luminescent properties of ZnO nanorod arrays grown at low temperature
J. Appl. Phys. **109**, 103508 (2011); 10.1063/1.3586243

Synthesis of In 2 O 3 nanocrystal chains and annealing effect on their optical properties
J. Vac. Sci. Technol. A **25**, 1038 (2007); 10.1116/1.2710244

Structural and optical properties of Si Si O 2 superlattices prepared by low pressure chemical vapor deposition
J. Appl. Phys. **100**, 013524 (2006); 10.1063/1.2210667

H-induced effects in luminescent silicon nanostructures obtained from plasma enhanced chemical vapor deposition grown Si y O 1 y : H (y > 1 3) thin films annealed in (Ar + 5 % H 2)
J. Vac. Sci. Technol. A **24**, 817 (2006); 10.1116/1.2177227

Defect-enhanced photoconductive response of silicon-implanted borosilicate glass
Appl. Phys. Lett. **85**, 935 (2004); 10.1063/1.1779945

Re-register for Table of Content Alerts

Create a profile.

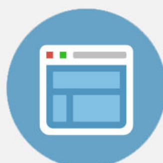

Sign up today!

[This article is copyrighted as indicated in the article. Reuse of AIP content is subject to the terms at: http://scitation.aip.org/termsconditions. Downloaded to] IP: 140.113.38.11 On: Thu, 01 May 2014 05:16:37

Effect of low-temperature annealing on the luminescent lifetime and negative differential resistance of silicon-implanted borosilicate glass

Gong-Ru Lin[a]
Institute of Electro-Optical Engineering, National Chiao Tung University, 1001, Ta Hsueh Road, Hsinchu, Taiwan 300, Republic of China

(Received 19 June 2003; accepted 10 October 2003)

The silicon-implanted borosilicate glass ($BSO:Si^+$) low-temperature (500 °C) annealed at a different time are structurally, electrically, and optically characterized. The weak and broadened x-ray diffraction reveal insignificant Si nano-crystallization even after long-term annealing, whereas the redshifted photoluminescence (PL) interprets the change in category and the decrease in density of irradiative defects in $BSO:Si^+$. Time-resolved PL analysis reveals a lengthening luminescent lifetime of $BSO:Si^+$ from 1.7 to 2.8 ns, which indicates that the density ratio of nonradiative defects in as-implanted $BSO:Si^+$ are reduced by one-tenth after annealing for 60 min. Transmission line mode analysis shows that both the leakage current and the contact resistance of a metal–$BSO:Si^+$–metal diode has dramatically changed by three orders of magnitude. A strong negative differential resistance (NDR) and associated double-barrier electron tunneling phenomenon are observed with a threshold electric field of 290–350 kV/cm. The decreasing barrier height of the metal–$BSO:Si^+$ junction from 3.0 to 1.9 eV is mainly contributed by deep-level defects with activation energy of ~1 eV. After annealing, the NDR effect significantly diminishes, the barrier height raises to >2.4 eV, and most electrical characteristics of the metal–$BSO:Si^+$ junction have recovered back to be comparable with those of the metal–BSO junction due to the elimination of these defects. © *2003 American Institute of Physics.* [DOI: 10.1063/1.1630366]

I. INTRODUCTION

Various fabricating technologies were developed in the past few years to synthesize the buried Si nanocrystal in glass, quartz, and thermal dioxide (SiO_2) layer on Si substrates, which have inspired enormous research on its structure, electrical, and optical properties due to its potential applications in optoelectronics.[1–5] The Si nanocrystal has been shown to exhibit relatively strong photo- and electroluminescence (PL and EL) from the blue-green to near-infrared wavelength region.[6] Recently, the synthesis of Si nanocrystals via Si ion implantation has also caused considerable interest.[7] Song *et al.*[8] have reported the redshift in PL of Si ion-implanted SiO_2 ($SiO_2:Si^+$) films from 470 to 600 nm after annealing. Gazecki *et al.* have demonstrated the refractive index analysis of planar optical waveguides formed upon $SiO_2:Si^+$.[9] The Si nanocrystal has been employed not only for fabricating light emitting and guiding devices, but also for nanocrystallite memory devices and photoconducting sensors. Not long ago, the inversion- and accumulation-mode gate current density of metal–oxide–semiconductor (MOS) capacitors with a 50-nm-thick $SiO_2:Si^+$ layer with doses from 10^{13} to $3\times10^{16}\,cm^{-2}$ have been studied.[10] The possible carrier transport mechanism has been referred to either as the Fowler–Nordheim (FN) or the Poole–Frenkel (PF) model.[11–13] Furthermore, Rossi *et al.*[14] has characterized optical and electrical properties of Si nanocrystals formed in continuous-wave argon-laser-treated and hydrogenated amorphous SiO_x alloys under different processing conditions. The thermionic conductivity of the $SiO_2:Si^+$ has indicated the existence of deep-level defects with an activation energy of $E_a\cong 1$ eV. Other anomalous electrical phenomena such as variable-range hopping conduction was also found in Si-implanted Si or porous Si materials containing Si nanostructures.[15,16] It was believed that the formation of Si nanocrystals could induce a dramatic change in the temperature dependence of the conductivity. In addition, the negative differential resistance (NDR) effect in, such as, SiO_x,[17] single porous Si layer,[18] porous Si supperlattice,[19] and Al_2O_3 matrix with buried Si nanocrystals,[20] have also been reported. The NDR-related resonant electron tunneling behavior has also been studied.[21–23] Nonetheless, the variation in the electrical properties of $SiO_2:Si^+$ annealed at low temperature conditions was less discussed in previous studies. In this article, the effect of low-temperature annealing on the defect-induced anomalous electrical characteristics of silicon-implanted borosilicate glass ($BSO:Si^+$) is studied via the transmission line model (TLM) analysis of metal-semiconductor metal (MSM) diodes with various spacing made on as-implanted and annealed $BSO:Si^+$ substrates. The evolution in the NDR effect as well as the electron tunneling behavior, the contact and sheet resistances, the breakdown field, the saturation current, and the barrier height of the MSM diode made on $BSO:Si^+$ annealed at different durations are reported.

II. EXPERIMENT

The $BSO:Si^+$ samples were prepared by multiple-energy implanting the 125 ± 20-μm-thick BSO glass with Si ions at energies of 50, 100, and 200 keV under the same dosage of

[a]Electronic mail: grlin@faculty.nctu.edu.tw

 © 2003 American Institute of Physics

[This article is copyrighted as indicated in the article. Reuse of AIP content is subject to the terms at: http://scitation.aip.org/termsconditions. Downloaded to] IP: 140.113.38.11 On: Thu, 01 May 2014 05:16:37

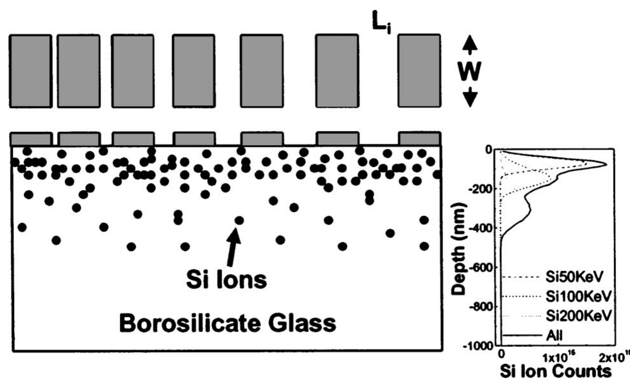

FIG. 1. The block diagram of the MSM diode for TLM analysis made on BSO:Si^+ and the depth-distribution profile of Si ions in BSO glass.

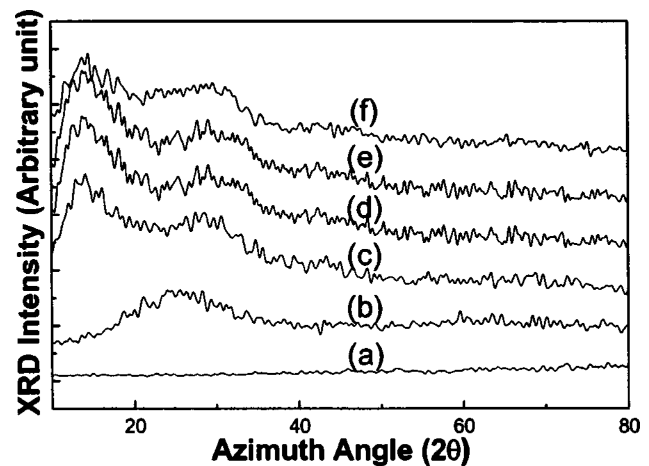

FIG. 2. The XRD analysis of (a) BSO glass, (b) as-implanted, (c) 30 min annealed, (d) 60 min annaled, (e) 90 min annealed, and (f) 120 min annealed BSO:Si^+ samples.

10^{16} ions/cm^2. The implanted depth profile of Si ions obtained by use of a Monte Carlo simulating program (TRIM) is shown in Fig. 1. The encapsulated thermal annealing of BSO:Si^+ samples was performed in a furnace with flowing nitrogen gas at 500 °C ranging from 30 to 120 min at 30 min increments. The structural property of the BSO:Si^+ is characterized by x-ray diffraction (XRD) with Cu $K\alpha$ radiation and room-temperature photoluminescence (PL) spectroscopy with an excitation wavelength of 360 nm. Nanosecond lifetime measurements are achieved by using a commercially available time-resolved PL (referred as TRPL) system, which consists of a pulsed nitrogen lamp as the 350 nm wavelength excitation source and a photon counter (Edinburgh, FL900). The TRPL system has the spectral range, the pulse width, and the repetition rate ranging from 110 to 850 nm, ~1 ns, and 40 kHz, respectively. The detection is performed by a cooled Hamamatsu GaAs photomultiplier tube (PMT) controlled at −22 °C. A time-correlated single-photon counting system is used to characterize the fluorescence lifetime of the BSO:Si^+ sample at a wavelength of 500 nm. To investigate the NDR effect, 200-nm-thick Al electrodes for TLM analysis were fabricated with contact size and spacing of 75×50 μm^2 and ranging from 1 to 25 μm, respectively. The current–voltage ($I-V$) measurements were performed using a programmable high-resistance meter (Hewlett Packard HP4339B), in which the biased voltage of the BSO:Si^+ MSM diode was scanned from 0 to 600 V at increments of 1 V. The entire scanning time for the $I-V$ profile is 6 s, which corresponds to a ramp rate of 0.1 V/ms. After measuring the resistances (R_i) of SiO_2:Si^+ diodes with different contact spacing (L_i), the lateral contact resistance (R_c) and the sheet resistance (R_s) can be evaluated from the intercept of $-2R_c w/R_s$ at the x axis and the intercept of $2R_c$ at the y axis in the plot of $R_i = 2R_c + R_s L_i/W$ as a function of L_i. The specific contact resistivity of the MSM diode made on BSO:Si^+, $\rho_c = W^2 R_c^2/R_s$ can also be obtained.

III. RESULTS AND DISCUSSIONS

The XRD curve of BSO glass is significantly changed after Si implantation, as shown in Fig. 2. The as-implanted BSO:Si^+ exhibits a relatively weak and broadened XRD peak at an azimuth angle of about 25° associated with its full-width at half-maximum (FWHM) of about 14°. After annealing for 30 min, the original XRD peal splits into two peaks located at angles of 14° and 29° with FWHM of 8° and 12°, respectively. The XRD peak at $2\theta = 29°$ is previously attributed to the recrystalization of (111)-oriented Si phases in the BSO:Si^+ glass.[17,18] The other XRD peak centered at $2\theta = 14°$ considerably correlates with the gradually crystallized SiO_2 matrices. Nonetheless, these XRD peaks reveal that the formation of Si nanocrystals is insignificant even after such a long-term annealing. On the other hand, the PL spectra of BSO:Si^+ samples prepared at different annealing times have revealed a redshift phenomenon, as shown in Fig. 3. Relatively broadened PL spectrum ranged from 450 to 550 nm is observed in the as-implanted BSO:Si^+ sample,[19–22] which is slightly enhanced with a central wavelength at 490 nm after 30 min annealing. These observations correlate well with those reported by Song[19] and Liao.[20] Such a short-wavelength PL signal has previously been attributed to either the contribution of the Si precipitates with subnanometer size (at least <1.4 nm),[4,2] or the spontaneous emissions of the nonbridging oxygen hole center (NBOHC, $O_3 \equiv Si-O$), or the $\equiv Si-Si \equiv$ based irradiative defects.[3] The size of such Si

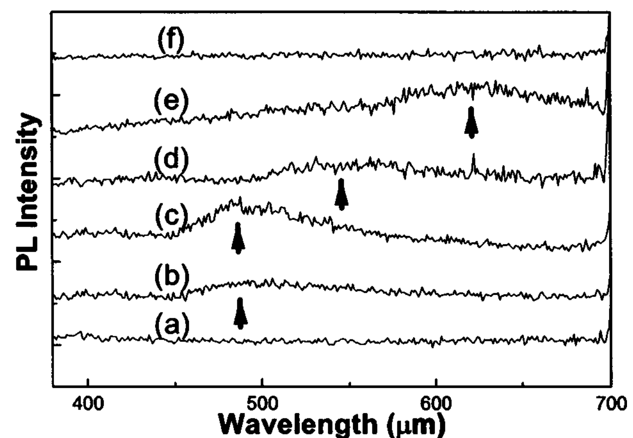

FIG. 3. The PL spectra of (a) BSO glass, (b) as-implanted, (c) 30 min annealed, (d) 60 min annealed, (e) 90 min annealed, and (f) 120 min annealed BSO:Si^+ samples.

[This article is copyrighted as indicated in the article. Reuse of AIP content is subject to the terms at: http://scitation.aip.org/termsconditions. Downloaded to] IP: 140.113.38.11 On: Thu, 01 May 2014 05:16:37

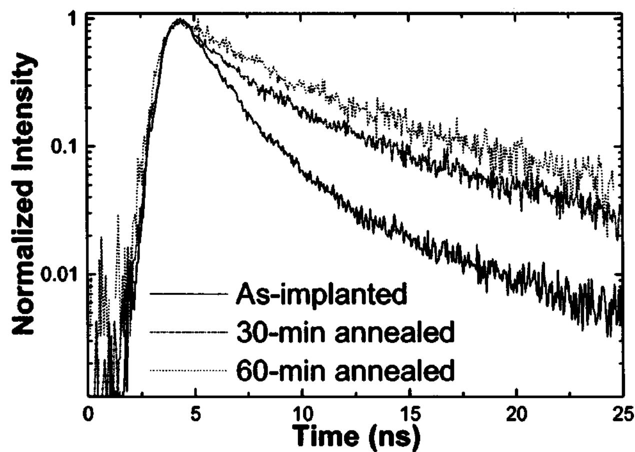

FIG. 4. The normalized TRPL traces of as-implanted (solid line), 30 min annealed (dash-dot line), and 60 min annealed (dotted line) BSO:Si^+ samples.

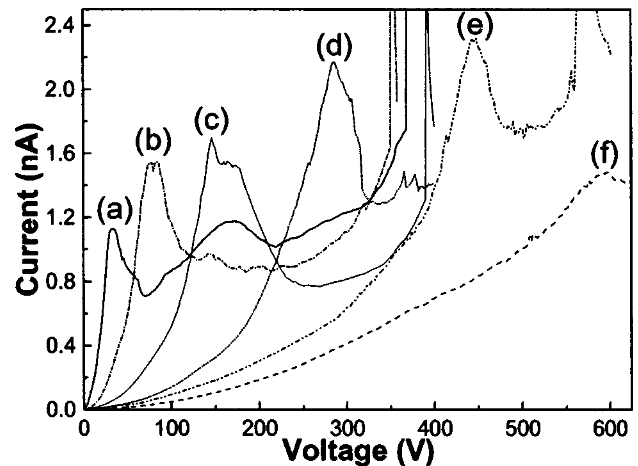

FIG. 5. The current–voltage of MSM diodes with contact spacing of (a) 1 μm, (b) 2.5 μm, (c) 5 μm, (d) 10 μm, (e) 15 μm, and (f) 20 μm fabricated on as-implanted BSO:Si^+ substrate.

precipitates has been roughly estimated as 0.8 nm by using Scherre's formula.[3,23] The PL of BSO:Si^+ redshifts to 500–600 nm and decays as the annealing time further lengthens. Nonetheless, the unchanged XRD peaks suggest that the size of Si nanocrystals may remain unchanged even after long-term annealing. These observations interpret that the contribution of the irradiative defects on the PL of BSO:Si^+ is more pronounced. The central PL peak further redshifts to 620 nm after 90 min annealing but eventually disappears as the BSO:Si^+ is annealed for up to 2 h. The decreasing PL intensity qualitatively confirms the elimination of the irradiative defects in BSO:Si^+ low-temperature annealed for longer durations.

In order to study the behavior of the nonradiative defect in BSO:Si^+, the TRPL analysis is performed and shown in Fig. 4. The carrier lifetimes of BSO:Si^+ is found to lengthen from 1.7 to 2.8 ns after annealing at 500 °C for 60 min or longer. A nonlinear least-squares-fitting reveals that the corresponding amplitudes and lifetimes of the two-step exponential decayed TRPL traces. In addition, other different fluorescence decay with a lifetime of 8.8–10.3 ns is also observed for as-implanted and annealed samples. The change of decay lifetime range is small. The decrease of nonradiative defect density of BSO:Si^+ by a factor of 2 has also been confirmed by the Schokley–Read–Hall (SRH) model. The secondary decayed lifetimes for the nonradiative defect in as-implanted, 30 min annealed, and 60 min annealed BSO:Si^+ samples are nearly identical, which indicates that the corresponding nonradiative defect (T_2) concentration is invariable. By using the SRH model under the assumptions of the unchanged capture cross section and carrier velocity, the first decayed lifetimes of the nonradiative defects in as-implanted, 30 min annealed and 60 min annealed samples are with a ratio of 1:1.2:1.6 which corresponds to a changing ratio in defect density of 1.7:1.4:1. These results interpret that the defect concentration is decreased by a factor of almost 2 after 1 h of annealing. According to the relative amplitude for the TRPL decayed components of the BSO:Si^+ sample at different annealing times, the density ratio of corresponding nonradiative defects (T_1) in as-implanted, 30 min annealed, and 60 min annealed BSO:Si^+ samples are 17.9:3:1.5. It is observed that the effect of thermal annealing on the elimination of T_1 defects is more pronounced than that of the T_2 defects. The vicissitude on the relative weighting factor of amplitudes corresponding to the faster and slower PL decays corroborates again the exchange in the contribution of these two nonradiative defects during the annealing process again.

The TLM diode with contact spacing of 2.5 μm made on the BSO glass exhibits a completely insulating property with a negligible leakage current of only 5 pA at a bias of up to 350 V, which further decreases down to <1 pA as the contact spacing enlarges. After implanting, the BSO glass is no longer insulating owing to the generation of dense defects, as shown in Fig. 5. The leakage current of the BSO:Si^+ diode with 2.5 μm contact spacing is found to change from 0.25 to 600 pA at a bias of 50 V, which further increases up to 1.5 nA and turns to breakdown at a bias of 350 V or larger. The TLM measurements indicate that the total resistance of the BSO glass has reduced by four orders of magnitude after Si-ion implantation.[23] At a bias of 20 V, the contact resistance, the sheet resistances, and the specific contact resistivity of the BSO glass decrease from $1.8\times10^{14}\,\Omega$, $2.3\times10^{15}\,\Omega/\square$, $7.7\times10^{8}\,\Omega\,\mathrm{cm}^2$ to $5.9\times10^{10}\,\Omega$, $8.6\times10^{12}\,\Omega/\square$, and $2.3\times10^{4}\,\Omega\,\mathrm{cm}^2$, respectively. In particular, the as-implanted BSO:Si^+ diode exhibits an anomalous current overshooting phenomenon. For example, the leakage current of a BSO:Si^+ diode with 1 μm contact spacing greatly overshoots to 1.1 nA at a bias of 33 V, which subsequently recovers back and overshoots again as the biased voltage increases up to 170 V. However, the secondary current overshooting behavior is relatively weak as compared to the first one. In comparison, the diode made on BSO glass only shows a linear current–voltage relationship before breakdown.[23] Such an anomalous carrier transport is known as the NDR phenomenon observed in a resonant tunneling diode made on conventional semiconductors. In general, the NDR results from the transfer electron effect observed in compound semiconductors, in which the hot electrons under

[This article is copyrighted as indicated in the article. Reuse of AIP content is subject to the terms at: http://scitation.aip.org/termsconditions. Downloaded to] IP: 140.113.38.11 On: Thu, 01 May 2014 05:16:37

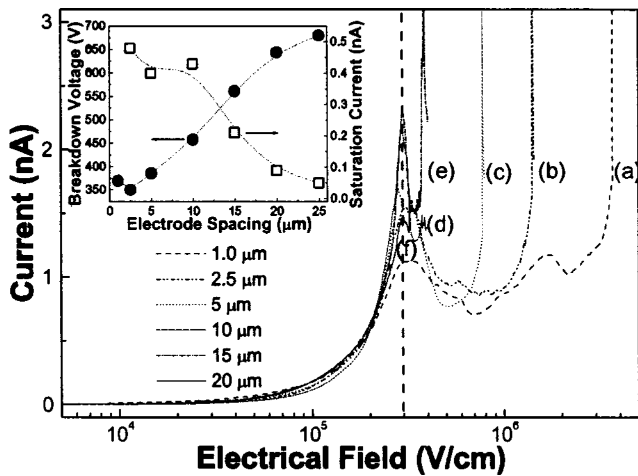

FIG. 6. The current-field characteristics of MSM diodes with contact spacing of (a) 1 μm, (b) 2.5 μm, (c) 5 μm, (d) 10 μm, (e) 15 μm, and (f) 20 μm fabricated on as-implanted BSO:Si^+ substrate. The inset figure plots the breakdown voltage and saturation current of these diodes as a function of contact spacing.

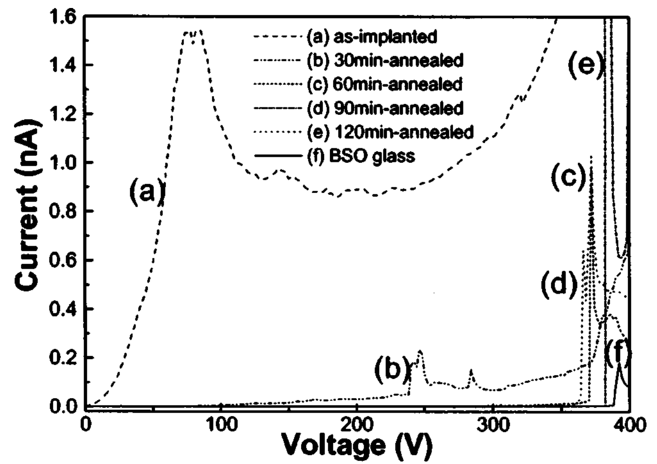

FIG. 7. The leakage current of a metal–BSO:Si^+–metal diode at different annealing times.

high electric field may exhibit higher kinetic energy to move from the central energy valley to the higher energy valley with heavier effective mass and lower drift velocity. Alternatively, the NDR can also be explained as the single or double barrier electron tunneling characteristic[24] of the MSM diode made on all kinds of semiconductors. Some of the similar results observed in porous[15] and amorphous[16] Si semiconductors have been explained as the contribution of dense localized states which also induce the hopping conduction effect. As the contact spacing enlarges, the first overshooting peak upper-shifts to larger biased voltage associated with a higher current level, while the secondary overshooting peak gradually diminishes. If we further plot the leakage current of the as-implanted BSO:Si^+ diode as a function of electric field strength, the threshold electric field for the NDR of the as-implanted BSO:Si^+ sample is obtained as 2.9–3.5 kV/cm, as shown in Fig. 3(right). This value is very close to that of the diode made on bulk GaAs substrate, and is far smaller than a GaN-based device (80–150 kV/cm).[25] The breakdown voltage of the as-implanted BSO:Si^+ diode increases from 350 to 680 V as the contact spacing enlarges from 1 to 25 μm, as shown in the inset of Fig. 6. Before breakdown, the saturation current (I_s) of the BSO:Si^+ diode with 2.5 μm contact spacing is determined as 0.48 nA, which linearly decreases by approximately one order of magnitude as the contact spacing enlarges to 25 μm. In more details, the barrier height of the metal–BSO:Si^+ junction can also be estimated if we consider the general formula of saturation current as

$$I_s = AA^*T^2e^{-q\phi_B/kT},$$

where A and A^* are the Richardson constants, T is the circumstance temperature, and ϕ_B is the barrier height in units of eV. The barrier height for the as-implanted BSO:Si^+ diode is about 1.9 eV, which is in good agreement with that measured by Kameda *et al.* using Fowler–Nordheim (FN) theory.[11] This is the primary observation of the NDR effect in the planar MSM diode fabricated on as-implanted BSO:Si^+ substrate, which strongly correlates with the dense defects induced by implantation rather than the Si nanocrystals.

After annealing for 30 min, the leakage current of the BSO:Si^+ diode is found to decrease by at least two orders of magnitude (see Fig. 7). The contact resistance, sheet resistance, and specific contact resistivity of the annealed BSO:Si^+ diode calculated from the TLM analysis also recovers back to be $1.01\times10^{14}\,\Omega$, $1.46\times10^{15}\,\Omega/\square$, and $3.93\times10^8\,\Omega\,cm^2$, which are comparable with the values of the same device made on BSO glass. The peak voltage for the weak current overshooting is found to upper-shift from 80 to 250 V. According to the double barrier tunneling theory, such a upper shift is mainly attributed to the increase in the barrier height of the metal–BSO:Si^+ junction. To confirm, we have calculated the barrier height at the interface of metal and annealed BSO:Si^+ from the diode saturation current, as shown in Fig. 8. Indeed, it is found that the barrier height of the metal–BSO:Si^+ junction is also found to increase from 1.92 to 2.1 eV after a 30 min annealing process. As the annealing time increases up to 60 min or larger, the leakage current of BSO:Si^+ is reduced to be comparable with that of the BSO glass. The disappearance of the NDR effect in the annealed BSO:Si^+ interprets that the Si-implanted defects

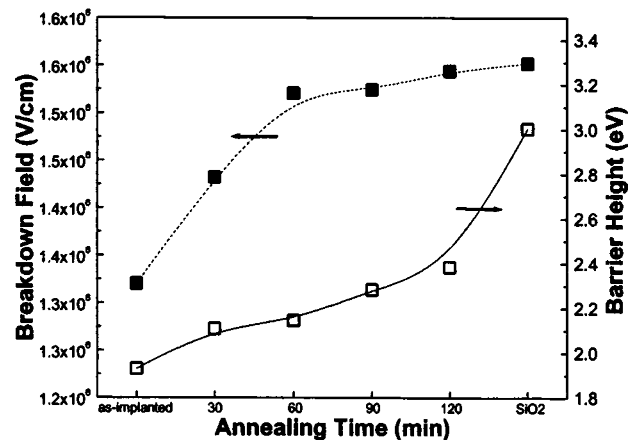

FIG. 8. The breakdown field strength (closed square) and the barrier height (open square) of a metal–BSO:Si^+ junction at different annealing times.

[This article is copyrighted as indicated in the article. Reuse of AIP content is subject to the terms at: http://scitation.aip.org/termsconditions. Downloaded to] IP: 140.113.38.11 On: Thu, 01 May 2014 05:16:37

have greatly reduced, which directly leads to an increase in barrier height of the metal–BSO:Si^+ junction. This recovery of barrier height during long-term annealing has also been verified in our experiments. In addition, the breakdown field of the BSO:Si^+ diode is also recovered from 1.32 to 1.55 MV/cm as the annealing time lengthens from 30 min to 2 h, which is very close to that of the same diode made on the unprocessed BSO glass. The associated barrier height is further increased to >2.4 eV, which becomes only 0.6 eV smaller than that of the metal–BSO glass junction. The long-term thermal annealing process degrades the defect enhanced electron tunneling mechanism in the as-implanted BSO:Si^+. Although some Si nanocrystals might be grown under the low-temperature and long-term annealing process, which is less contributed to the electrical properties of the BSO:Si^+ substrate based on our experimental observations.

IV. CONCLUSIONS

In conclusion, the effect of annealing time on the defect-induced anomalous electrical characteristics of low-temperature (500 °C) annealed silicon-implanted borosilicate glass (BSO:Si^+) has been optically and electrically characterized. The weak and broadened XRD peaks reveal the insignificant formation process of sub-nm Si clusters even after long-term annealing, whereas the redshifted PL spectra confirm the change in category and the decrease in density of irradiative defects in BSO:Si^+. The carrier lifetimes of BSO:Si^+ are found to lengthen from 1.7 to 2.8 ns after annealing at 500 °C for 60 min or longer. The density ratio of corresponding nonradiative defects (T_1) in as-implanted, 30 min annealed, and 60 min annealed BSO:Si^+ samples are 17.9:3:1.5. The TLM analysis reveals the dramatic changes in both the leakage current and the contact resistance of as-implanted BSO:Si^+ by at least three orders of magnitude. the diode made on as-implanted BSO:Si^+ exhibits strong current overshooting and rectified characteristics, however, which diminish after a long-term annealing process. The overshooting voltage linearly increases as the diode contact spacing increases. The NDR phenomenon with a threshold electric field of 2.9–3.5 kV/cm and the associated double-barrier electron tunneling behavior are also observed. After implanting, the decrease in barrier height of the metal–BSO glass junction from 3.0 to 1.9 eV correlates well with the contribution of the deep-level defects with an activation energy of nearly 1 eV. After annealing for 30 min or longer, the leakage current and contact resistance of the metal–BSO:Si^+ junction recovers back to be comparable with those of the metal–BSO glass junction. The NDR effect gradually diminishes and the barrier height increases up to >2.4 eV (2 h annealed). These observations conclude the more pronounced contribution of the defects (as compared to Si nanocrystals) in the anomalous carrier transport of BSO:Si^+.

ACKNOWLEDGMENTS

This work was supported in part by the National Science Council (NSC) of the Republic of China under Grant No. NSC 91-2215-E-009-039. Technical support of this work by Optical Science Center at National Central University is also appreciated. The author thanks Chin-Chia Hsu for his effort in some of the experiments.

[1] S. Tiwari, F. Rana, H. Hanafi, A. Hartstein, E. Crabbe, and K. Chan, Appl. Phys. Lett. **68**, 1377 (1996).
[2] K. D. Hirschman, L. Tsybeskov, S. D. Duttagupta, and P. M. Fauchet, Nature (London) **384**, 338 (1996).
[3] Y. Kanemitsu, Phys. Rep. **263**, 1 (1995).
[4] M. L. Brongersma, K. S. Min, E. Boer, T. Tambo, A. Polman, and H. A. Atwater, Mater. Res. Soc. Symp. Proc. **486**, 275 (1998).
[5] S. Hayashi, T. Nagareda, Y. Kanzawa, and K. Yamamoto, Jpn. J. Appl. Phys., Part 1 **32**, 3840 (1993).
[6] L. Rebohle, J. Borany, R. A. Yankov, W. Skorupa, I. E. Tyschenko, H. Frob, and K. Leo, Appl. Phys. Lett. **71**, 2809 (1997).
[7] G. H. Li, K. Ding, Y. Chen, H. X. Han, and Z. P. Wang, J. Appl. Phys. **88**, 1439 (2001).
[8] H. Z. Song, X. M. Bao, N. S. Li, and J. Y. Zhang, J. Appl. Phys. **82**, 4028 (1997).
[9] J. Gazecki, J. M. Kubica, M. Zamora, G. K. Reeves, C. M. Johnson, and M. C. Ridgway, Thin Solid Films **340**, 233 (1999).
[10] M. Y. Hao, H. Hwang, and J. C. Lee, Appl. Phys. Lett. **62**, 1530 (1993).
[11] E. Kameda, T. Matsuda, Y. Emura, and T. Ohzone, Solid-State Electron. **42**, 2105 (1998).
[12] A. Kalnitsky, A. R. Boothroyd, and J. P. Ellul, Solid-State Electron. **33**, 893 (1990).
[13] R. D. Gould and M. G. Lopez, Thin Solid Films **343–344**, 94 (1999).
[14] M. C. Rossi, S. Salvatori, M. Burchielli, and G. Conte, Thin Solid Films **383**, 267 (2001).
[15] A. I. Yakimov, N. P. Stepina, and A. V. Dvurechenskii, J. Phys.: Condens. Matter **6**, 2583 (1994).
[16] E. Lampin, C. Delerue, M. Lannoo, and G. Allan, Phys. Rev. B **58**, 12044 (1998).
[17] M. G. Lopez and R. D. Gould, Thin Solid Films **254**, 291 (1995).
[18] S.-J. Wang, J.-C. Lin, and H. Y. Tsai, Electron. Lett. **32**, 1618 (1996).
[19] M.-K. Lee, C.-H. Chu, Y.-C. Tseng, J.-M. Shyr, and C.-H. Kao, IEEE Electron Device Lett. **21**, 587 (2000).
[20] Q. Wan, N. L. Zhang, X. Y. Xie, T. H. Wang, and C. L. Lin, Appl. Surf. Sci. **191**, 171 (2002).
[21] G. Y. Xu, M. Liu, X. S. Wu, Y. L. He, and T. M. Wang, J. Phys.: Condens. Matter **11**, 8594 (1999).
[22] L. Tsybeskov *et al.*, Europhys. Lett. **55**, 552 (2001).
[23] G.-R. Lin, Jpn. J. Appl. Phys., Part 2 **41**, L1379 (2002).
[24] O. Pinaud, J. Appl. Phys. **92**, 1987 (2002).
[25] E. Alekseev and D. Pavlidis, Solid-State Electron. **44**, 941 (2002).

[This article is copyrighted as indicated in the article. Reuse of AIP content is subject to the terms at: http://scitation.aip.org/termsconditions. Downloaded to] IP: 140.113.38.11 On: Thu, 01 May 2014 05:16:37